

Enhanced Proton Conductivity of Cerium Induced Tin Phosphate Cation Exchange Material

VINISHA VALSARAJ P¹, JANARDANAN C.

¹Research and Post Graduate Department of Chemistry, Sree Narayana College, Kannur, Kerala-670 007, INDIA Email:- vinipunep@gmail.com, jeeje_dianthus@yahoo.com

Abstract

Tin phosphate cation exchange material was prepared by simple precipitation method. Cerium was introduced in the matrix of tin phosphate by co-precipitation techniques. The ion exchange capacity, chemical stability, and pH titration studies were carried out to understand the ion exchange capability. The physico-chemical characterization was studied by elemental analysis, XRD, FTIR and TGA. The presence of protons makes the tetravalent metal acid salt, a potential candidate for solid state protonic conduction. In the present endeavour, the proton conduction behaviour of tin phosphate and cerium induced tin phosphate has been studied by measuring specific conductance (S) at different temperatures in the range 30–80°C using Solatron (1255B FRA F11287 Electrochemical Phase) impedance analyzer.

Keyword: Cation exchanger, proton conduction, tetravalent metal acid salts, tin phosphate,

Introduction

In recent years there are lot of research work, focused at developing new proton conductors and determining their conduction mechanism, which makes its potential use in the field of fuel cell, sensors, water electrolysis units and other electrochemical devices. Fast proton conduction is often observed in inorganic ion exchange materials which contain high valent cations^{1,2}. Inorganic metal phosphates having general formula $M(IV)(HPO_4) \cdot nH_2O$ possess interesting properties like protonic and alkali metal conductivity^{1,2}, catalytic³, and ion-exchange^{4,5}. These metal phosphates possess structural hydroxyl protons that are responsible for their ion-exchange behaviour. The number of protons present in the structural hydroxyl groups indicates its potentiality to exhibit as solid state proton conductor. When these –OH groups are hydrated, the protons can move easily on the surface, thus accounting for their conductivities, which depend strongly on relative humidity, surface area and degree of crystallinity⁶. Alberti and co-workers have shown that the protons on the surface conduct a thousand times faster than protons through bulk⁷.

The diffusion and proton transport mechanism in crystalline zirconium phosphate and titanium phosphate has been reported by various workers⁷⁻¹⁶. An early study on zirconium phosphate with varying crystallinity depicts the importance of degree of crystallinity in the proton conduction^{7,17,18}. Stenina and co-workers have reported the conduction behaviour of tin phosphate¹⁹. Literature survey reveals that most

of the proton transport properties carried out in case of zirconium phosphate and titanium phosphate and not many report in the case of tin phosphate. Conductivity of lithium exchanged tin phosphate and zirconium phosphate have been reported. In the light of above factor, in the present endeavor, we have studied the protonic nature of cerium induced tin phosphate. These materials have been characterized for elemental analysis (ICP-AES), thermal analysis (TGA), X-ray analysis and FTIR spectroscopy. Chemical resistivity of these materials has been accessed in acidic, basic and organic solvent media. The transport properties of these materials has been explored by measuring specific proton conductance at different temperatures in the range 30–80°C at 10°C intervals, using a Solartron Dataset impedance analyser (SI 1260) over the frequency range 5 Hz–1 MHz at a signal level below 1V.

Material and methods

Reagents

Stannic chloride (E.Merck), ammonium ceric nitrate (E.Merck) and sodium dihydrogen phosphate (E.Merck) were used for the synthesis of the exchangers. All other reagents and chemicals used were of analytical grade.

Apparatus and instruments

A glass column was used for column operations. ELICO LI613 pH meter was used for pH measurements. Chemical composition was determined by ICP-AES method using ICP-AE Spectrometer Thermo Electron IRIS Intrepid II. FT-IR Spectrometer model Thermo-Nicolet Avtar 370 for IR studies, X-ray Diffractometer Bruker AXS D8 Advance for X-ray diffraction studies were used. UV Solatron (1255B FRA FI1287 Electrochemical Phase) impedance analyzer was used for conductivity measurements. Perkin Elmer Diamond TG/DTA Analysis System for thermal analysis and an electric shaking machine for shaking were also used.

Synthesis of the exchanger

Tin phosphate (SnP): Stannic chloride solution (0.05 M) and sodium dihydrogen phosphate solution (0.05 M) were prepared. Sodium dihydrogen phosphate solution was added to stannic chloride solution with constant stirring in different volume ratios so that final volume was 500 mL. The resulting gel was kept for 24 hrs at room temperature maintaining the pH at 1 with 1.0 M NaOH/1.0 M HNO₃. It was then filtered, washed with deionized water and dried. The exchanger was then converted into the H⁺ form by treating with 1.0 M HNO₃ for 24 hrs with occasional shaking and intermittent changing of acid. It was then washed with deionized water to remove the excess acid, dried and sieved to obtain particles of 60-100 mesh.

Tin cerium phosphate (SnCeP): Ammonium ceric nitrate solution (0.05 M), stannic chloride solution (0.05 M) and sodium dihydrogen phosphate solution (0.05 M) were prepared. Sodium dihydrogen phosphate solution was added to mixtures of ammonium ceric nitrate solution and stannic chloride

solution with constant stirring in different volume ratios so that final volume was 500 mL. The resulting gel was kept for 24 hrs at room temperature maintaining the pH at 1 with 1.0 M NaOH/1.0 M HNO₃. It was then filtered, washed with deionized water and dried. The exchanger was then converted into the H⁺ form by treating with 1.0 M HNO₃ for 24 hrs with occasional shaking and intermittent changing of acid. It was then washed with deionized water to remove the excess acid, dried and sieved to obtain particles of 60- 100 mesh.

Table -1: Specific Conductance of SnP and SnCeP at Various Temperatures

Temperature (K)	Specific conductivity σ (Scm ⁻¹)	
	SnP	SnCeP
303	1.35×10^{-4}	6.50×10^{-4}
313	1.88×10^{-4}	7.08×10^{-4}
323	2.42×10^{-4}	7.48×10^{-4}
333	3.15×10^{-4}	8.37×10^{-4}
343	3.56×10^{-4}	9.42×10^{-4}
353	5.04×10^{-4}	1.04×10^{-3}
Ea/kcalmol ⁻¹	5.52	0.89

Ion exchange capacity (IEC)

The ion exchange capacity of the material was determined by column method. 1.0 g of the exchanger in H⁺ form was taken in a glass column of 1.1 cm diameter. The H⁺ ions were eluted by percolating 100 mL of 1.0 M NaCl solution. The effluent was collected and titrated against standard sodium hydroxide solution. The ion exchange capacity, IEC in meqg⁻¹ was calculated using the formula,

$$IEC = \frac{av}{w}$$

Where, a is the molarity, v is the volume of alkali used during titration and, w is the weight of the exchanger taken²⁰.

Chemical resistivity

The chemical resistivity of the sample was assessed in mineral acids like HCl, HNO₃ and H₂SO₄, bases like NaOH and KOH and organic solvents like acetic acid, acetone, ethanol and diethyl ether. For this, 0.5 g of the sample was soaked in 50 mL of different solvents, kept for 24 hrs and changes in colour, nature and weight of the sample were noted.

Effect of temperature on IEC

The effect of temperature on ion exchange capacity was studied by heating several 1.0 g samples of the exchanger at different temperatures for 2 hrs in an air oven and Na⁺ ion exchange capacity in meqg⁻¹ was determined by the column method after cooling them to room temperature.

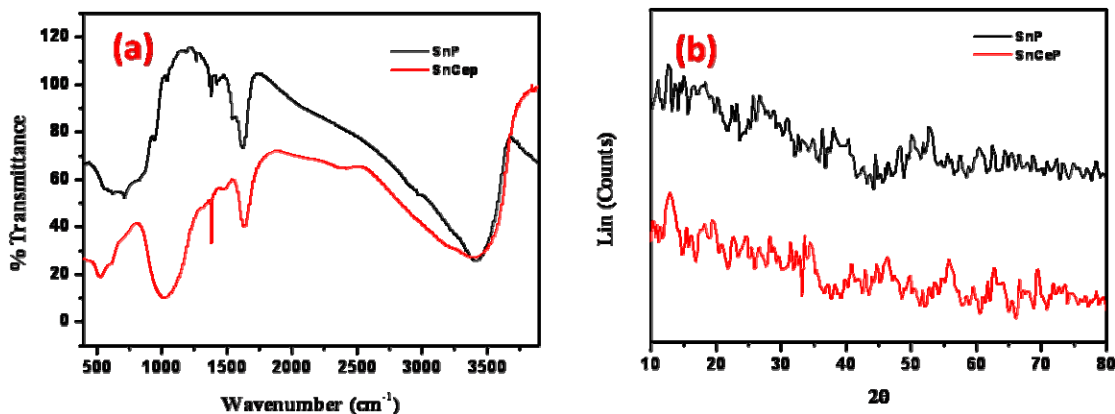


Figure (1a): FTIR spectra of SnP and SnCeP, and (1b) XRD of SnP, and SnCeP,

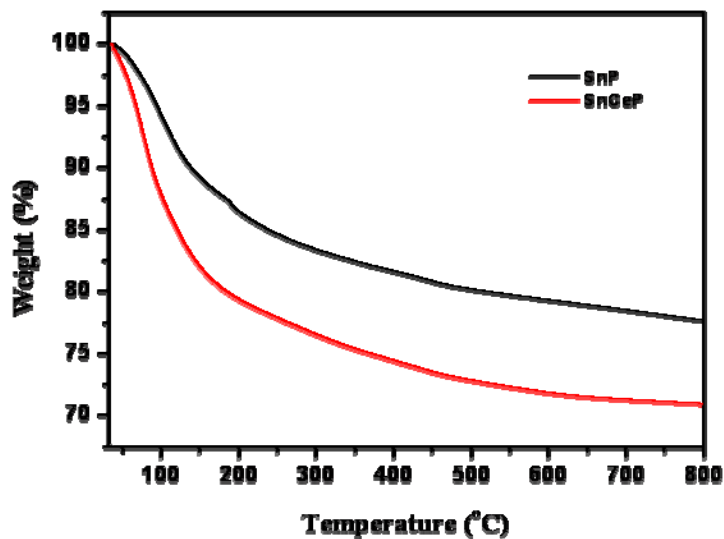


Figure 2: TGA of SnP and SnCeP

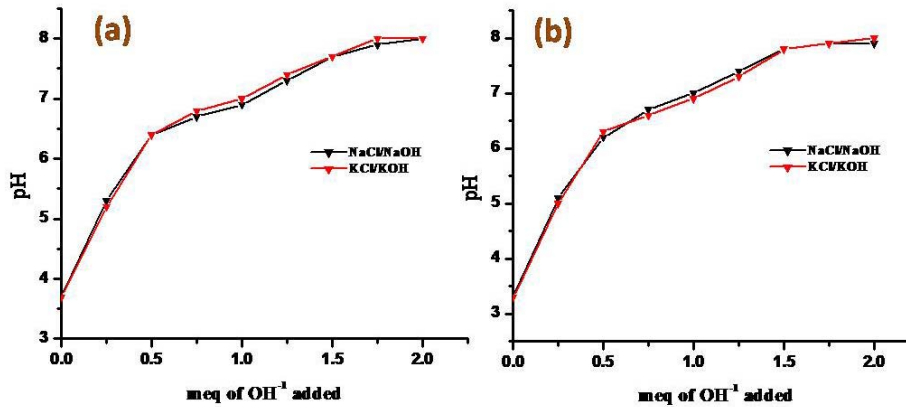


Figure 3: pH titration curve for (a) SnCeP and (b) SnP

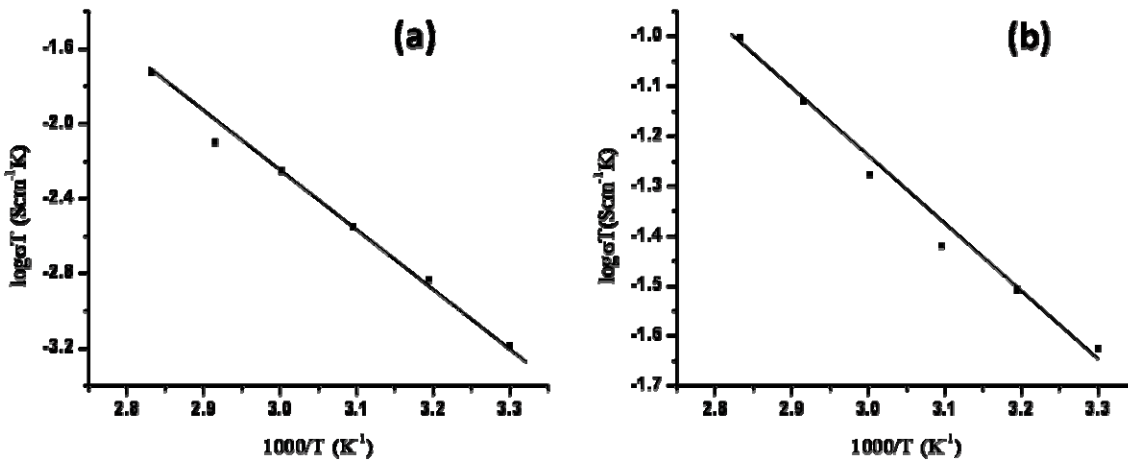


Figure 4: Arrhenius plot for (a) SnP and (b) SnCeP in the temperature range of 30–80 °C

pH titrations

Topp and Pepper method²¹ was used for pH titrations using NaOH/NaCl, KOH/KCl, systems. 0.5 g of exchanger was equilibrated with varying amounts of metal chloride and metal hydroxide solutions. At equilibrium (after equilibration), pH of the solutions was measured and plotted against the milliequivalents of OH⁻ added.

Conductivity measurements

The protonic conductivities of the materials were measured using pellets of 13 mm diameter and 1×5–2 mm thickness. The opposite sides of the pellets were coated with conducting silver paste to ensure good electrical contact. Impedance measurements were taken using 1255B FRA FI1287 Electrochemical Phase impedance analyser over a frequency range of 5 Hz to 1 MHz at a signal level below 1 V, interfaced to a minicomputer for data collection. The measurements were made in the temperature range 30–80 °C. In all

cases, since the impedance plots of the materials consist of single depressed semi-circles, the pellet conductivity was calculated by arc extrapolation to the X-axis, taking into account the geometric size of the pellets.

Results and discussion

The exchanger, synthesized SnP obtained as colourless transparent solid and SnCeP obtained as colourless transparent solid. It exhibit good chemical stability in water, acetic acid, 2.0 M NaOH, 2.0 M KOH, 15 M HNO₃, 10 M HCl and 20 M H₂SO₄. Elemental analysis by ICP-AES revealed tin, cerium, phosphorous ratio of 1: 1: 2.9 for SnCeP and ratio of tin and phosphorous for SnP is 1: 3 respectively. Na⁺ ion exchange capacity have been evaluated at room temperature and found to be SnP, 1.0 meqg⁻¹ and SnCeP, 1.15 meqg⁻¹.

FTIR spectra of SnCeP, and SnP (Figure 1a) showed a broad band in the region ~3444 cm⁻¹ which was assigned to symmetric and asymmetric -OH stretching, while the band at ~1633 cm⁻¹ was attributed to H-O-H bending. A band in the region ~1039 cm⁻¹ was attributed to P=O stretching. A band at ~1384 cm⁻¹ was an evidence for the presence of δ (POH). This indicated the presence of structural hydroxyl protons in SnCeP, which was more evident from the obtained IEC values, whereas in the case of SnP there was no prominent peak in that region. Bands at ~615 cm⁻¹ and ~516 cm⁻¹ may be due to the presence of Ce-O and Sn-O bonds.

There was no prominent peak in the x-ray diffractograms of SnP and SnCeP which suggested its amorphous nature of the materials (Figure 1b).

The thermogram of SnCeP cation exchanger (Figure 2) showed that the weight loss (about 20%) of the ion exchanger up to ~147 °C is due to the removal of free external water molecules²². Further, a gradual loss of mass (about 8%) up to 500 °C may be due to the condensation of hydroxyl groups. Above 500 °C, the gradual loss in weight (about 3%) up to 800 °C was due to the removal of structural water. There was no sudden decrease in the weight loss which indicated that there was no structural change of this material. The percent weight loss with increasing temperature observed by TGA curve for SnCeP and SnP. The nature of the degradation of SnP was similar like SnCeP but the percentage of weight loss was different for these materials. The percentage of weight loss was in the order SnCeP > SnP.

The two materials showed only one inflection point in the pH titration curves which confirm the monofunctional behaviour of the materials (Figure 3a and 3b). pH value of SnP and SnCeP when no OH⁻ ions were added to the system is that 3.30 and 3.20 which suggest the high acid nature of the materials.

Impedance measurements

In complex impedance plots for SnP and SnCeP at 303 K, impedance spectra consist of a single depressed semicircle. Sample resistance (R) was measured by extrapolation of high frequency arc crossing to Z axis. Proton conductivity was measured using eq, $\sigma = l/RA$, where σ is conductivity, l is sample thickness and

A is electrode area (cm^2). Arrhenius plot ($\log \sigma T$ vs $1/T$) are represented for SnP, and SnCeP. Activation energy for each sample was calculated using Arrhenius equation [$\sigma = \sigma_0 \exp(-E_a/kT)$] where k is Boltzmann constant and T is temperature.

Proton transport includes, transport of proton and any assembly that carries protons. Transport of protons between relatively stationary host anions is termed Grotthuss or free proton mechanism, which requires close proximity of water molecules, that are firmly held but able to rotate. The low value of E_a depicts that it depends entirely on reorientation step. Transport by other species is called as vehicle mechanism. Here polyatomic ion migrates as entities through bulk materials. Hence E_a is expected to be high. Vehicle mechanism is most frequently observed in aqueous solution and other liquid/melts. Vehicle mechanism is usually restricted to materials with open structures to allow passage of large ions and molecules in solids. The compounds which contain less amount of water would be expected to conduct by vehicle mechanism; in this a nucleophilic group acts as a proton carrier.

Conductivity measured in the range 30–80°C for SnP and SnCeP is presented in table 2. As calculated from the electron impedance spectra, sample SnP and SnCeP achieved a proton conductivity of 1.35×10^{-4} and $6.50 \times 10^{-4} \text{ S cm}^{-1}$ respectively at 90% relative humidity at 30°C. Arrhenius plots are presented in Figures 4a and 4b. For two materials linearity is observed in the temperature range 30–80°C. From specific conductance for SnP, and SnCeP, it is observed that increases with increasing temperature (Table 1). This fact is also supported by the study of heating effect on IEC, suggesting mechanism of transportation to be Grotthuss type, where conductivity depends on water ability located on the surface to rotate and participate. Further results are also in agreement with the suggestion that the protons are not able to diffuse along an anhydrous surface, where spacing of $-\text{OH}$ groups is too high. Although all the conductivities shown here increase with increasing temperature, the absolute values of the conductivity clearly vary with each other. The proton migration is dominantly through the Grotthuss mechanism. In this mechanism, the proton transport is mainly caused by the hopping of the protons from one water molecule to another through tunnelling mechanism. To a smaller extent, the proton forms hydrogen bond with the water molecules and exits as H_3O^+ and diffusion of H_3O^+ ions enhances the proton transport. The increase in temperature strongly affects both mechanisms; hopping as well as diffusion becomes faster. The activation energy for the proton migration was calculated and found to be 3.7 kJ mol^{-1} , which is in the range of activation energy for Grotthuss mechanism.

The higher conductivity value of SnCeP compared with SnP can correlate with the IEC value of these materials. Higher IEC values indicate more exchangeable protons and hence more available conducting protons. It is in agreement with the pH value of the exchangers. σ_{SnCeP} is higher compared to σ_{SnP} , may be attributed to some structural changes due to the presence of electron rich cerium ions. However, observed conductance depends on concentration of charge carriers, availability of vacant sites, crystal

structure, surface morphology, hydrophobicity, presence of interstitial sites, temperature, activation energy etc.

The energy of activation (E_a , kcalmol⁻¹) values observed are 5.52 for SnP and 0.89 for SnCeP. The activation energy at saturated humidity was less which means the lower energy barrier for the proton conduction. Therefore, both observations indicate that water molecule adsorbed by the mixed material promotes proton conduction to a high degree. This is mainly due to the adsorbed water molecules to form the proton channels in the interlayers of inorganic matrix for the smooth transfer of protons. E_a values follows the order SnCeP < SnP however σ values follows the order SnP < SnCeP. It shows that it has no correlation with the order of conductivity of the exchanger presented. The materials SnP and SnCeP synthesized in our lab have higher specific conductance compared with other materials discussed in the previous literatures.

Conclusion

In the present study, the proton transport properties of tin phosphates exhibit higher conductance compared to reported tin phosphate. Cerium incorporated tin phosphate shows enhanced proton conduction compared to tin phosphate. A study of transport properties of cerium induced tin phosphate would throw more light on the present investigation. The study clearly reveals that modifying the number of surface protons, results in an enhanced conduction. The materials presented in this paper have higher proton conductivity compared to other materials already reported; hence it will be a promising candidate in the field of electrochemical devices.

Acknowledgments

Author gratefully acknowledges the Council of Scientific and Industrial Research (CSIR), New Delhi, for the award of senior research fellowship. Instrumental support received from STIC, Kochi is also gratefully acknowledged.

Reference

- [1] G.Alberti, M.Casciola, Solid State Ionics., 2001, 145, 3-16.
- [2] R.Llavona, M.Suarez, J.R.Garcia, J.Rodriguez, Inorg. Chem., 1989, 28, 2863-2868.
- [3] G.Centi, F.Trifiro, J.R.Ebner, V.M.Franchetti, Chem. Rev., 1988, 88, 55-80.
- [4] G.Cao, H.G.Hong, T.E.Mallouk, Accounts Chem. Res., 1992, 25, 420-427.
- [5] A.Clearfield, Chem. Rev., 1988, 88, 125-148.
- [6] A.Clearfield, J.R.Berman, J. Inorg. Nucl. Chem., 1981, 43, 2141-2142.
- [7] G.Alberti, M.Casciola, U.Costantino, G.Levi, G.Riccardi, J. Inorg. Nucl. Chem., 1978, 40, 533-537.
- [8] G.Alberti, M.Casciola, U.Costantino, G.Radi, Gazz. Chim. Ital., 1979, 109, 421.
- [9] S.Yamanaka, J. Inorg. Nucl. Chem., 1980, 42, 717-720.



- [10] A.Clearfield, P.Jerus, Solid State Ionics., 1982, 6, 79-83.
- [11] J.P.Boilot, P.Barboux, D.Carrier, K.Lhalil, M.Moreau, Solid State Ionics., 2003, 185, 162
- [12] G.Alberti, Study week on biological and artificial membranes and desalination of water (ed.) R Passino (Vatican City: Pontificia Acad. Sci. Scr.Varia:) 1976, 40, 629.
- [13] A.T.Howe, M.G.Shelton, J. Solid State Chem., 1979, 28, 345-361.
- [14] G.Alberti, M.Bracardi, M.Casciola, Solid State Ionics., 1982, 7, 243-247.
- [15] L.Szirtes, E.Kuzmann, J.Megyeri, Z.Klencsar, Solid State Ionics., 2001, 145, 257-260.
- [16] L.Szirtes, J.Megyeri, L.Riess, E.Kuzmann, Solid State Ionics., 2003, 162–163, 181-184.
- [17] R.P.Hamlem, J. Electrochem. Soc., 1962, 109, 746-749.
- [18] G.Alberti, E.Torracca, J. Inorg. Nucl. Chem., 1968, 30, 1093-1099.
- [19] I.A.Stenina, A.D.Aliev, I.V.Glukhov, F.M.Spiridonov, A.B.Yaroslavtsev, Solid State Ionics., 2003, 162–163, 191-195.
- [20] A.I.Vogel, “A text book of quantitative inorganic analysis”, Longman Group Limited, London, 1975
- [21] N.E.Topp, K.W.Pepper, J. Chem. Soc., 1949, 690, 3299-3303.
- [22] S.A.Nabi, Mu.Naushad, Colloids Surf. A: Physicochem. Eng. Aspects., 2008, 316, 217-225.
- [23] B.Beena, U.Chadusama, Bull. Mater. Sci., 1996, 19, 405-409